THE JOURNAL OF PHYSICAL CHEMISTRY C

ARTICLE

pubs.acs.org/JPCC

Identifying the Numbers of Ag Atoms in Their Nanostructures Grown on a Si(111)-(7 × 7) Surface

Fangfei Ming,[†] Kedong Wang,[†] Xieqiu Zhang,[†] Jiepeng Liu,[†] Aidi Zhao,[‡] Jinlong Yang,[‡] and Xudong Xiao*[,†]

[†]Department of Physics, The Chinese University of Hong Kong, Shatin, New Territory, Hong Kong, China

[‡]Hefei National Laboratory for Physical Sciences at Microscales, University of Science and Technology of China, Hefei, Anhui 230026, China

ABSTRACT: Using scanning tunneling microscopy, we have conducted an in situ study of the room-temperature growth of Ag structures on a Si(111)-(7 × 7) surface. By observing the STM images at various Ag coverages, a number of Ag structures were identified in both the faulted and the unfaulted half unit cells. The number of Ag atoms contained in each of these Ag structures was precisely determined through observation of inter-half unit cell diffusion. Transformations between the Ag structures via inter- and intra-half unit cell diffusion provide detailed information for the mechanisms of Ag structure growth. The precision knowledge of the number of atoms in such structures will form a fundamental base for understanding the physical and chemical properties of these structures.

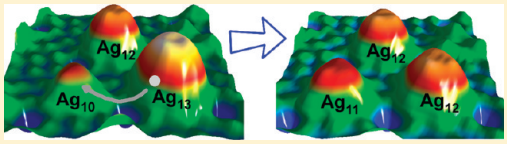

INTRODUCTION

During the past 20 years, metal nanostructures have been a central area of research in physics and chemistry.[1−6] Various physical properties of metal clusters have been investigated, with examples including the melting point of Na_{70-200},[7,8] the stability of Na_8[9] and Au_{20},[10] the optical property of Au_{5-31}[11] and Ag_8,[12] the magnetism of $Co_{12<n<200}$,[13] VCs_{1-12}, and VNa_{1-12},[14] and the geometries and electronic structures of V_{6-23},[15] Mg_{1-80},[16] $Cu/Ag/Au^-_{53-58}$,[17] Ag_{5-127},[18] $Na_{19,40,55,58,147}$,[19] Au_{2-20},[20,21] and $TiNa_{1-13}$.[22] Some have further examined the chemical properties of the metal clusters, such as the chemical reaction of Al^-_{7-60} with water,[23,24] $CuAl^-_{11-34}$ with O_2,[25] and the catalytic action of Au clusters.[26−28] In these studies, the number of atoms was often found to play a critical role in the properties of the clusters; e.g., among the Al anion clusters of Al^-_{7-60}, only $Al^-_{16,17,18}$ shows a remarkable larger reactivity with water to produce H_2.[23]

The demand for fabricating metallic nanoclusters with unique properties has also stimulated the recent studies on the processes and mechanisms of the initial growth of a number of metallic materials on semiconductor substrates. Ag on a Si(111)-(7 × 7) reconstruction surface is one of the most popular metal/semiconductor systems.[29−37] One reason is its low reactivity and intermixing at low temperatures.[29] Another is that the Si(111)-(7 × 7) surface has a large unit cell (∼2.7 nm), which consists of a faulted half unit cell (FHUC) and an unfaulted half unit cell (UHUC).[38] These half unit cells (HUCs) form identical atom traps for Ag atoms, leading to the formation of Ag clusters.[30,34,35,39] Previous experimental and theoretical works have shown the growth behavior of Ag on a Si(111)-(7 × 7) surface in terms of the occupancy and occupancy preference between FHUC and UHUC.[34,40] The adsorption and diffusion of a single Ag atom,[41−43] the adsorption site of two Ag atoms,[44] and the rectification behavior of a three Ag atom cluster[45] on Si(111)-(7 × 7) have also been well studied, uncovering rich physics in this system. These results further inspire our interest in Ag nanostructures with more atoms.

In this paper, we report our recent results on the configuration and the number of Ag atoms in various Ag nanostructures grown on Si(111)-(7 × 7) at room temperature. While there were a few reports on identical metal clusters consisting of more than three atoms fabricated on Si(111)-(7 × 7) at elevated temperatures,[46−48] the identification of the number of atoms in such clusters was rather indirect, remaining to be an issue in debate. To overcome the difficulties in the identification of the various kinds of structures and the determination of the number of atoms in the Ag structures on Si(111)- (7 × 7) from scanning tunneling microscopic (STM) images, we obtained a movie of the growth process by conducting several in situ deposition-imaging cycles on the same area of the Si(111)-(7 × 7) surface. Various kinds of isolated Ag structures containing up to 13 Ag atoms were then identified from the STM images. Structures with more than two Ag atoms were found to have almost identical configurations in FHUCs and UHUCs. From the recorded diffusion events of Ag atoms between HUCs, we have unambiguously identified the number of Ag atoms in these structures.

EXPERIMENT

Our experiments were carried out with an Omicron variable-temperature STM, which is operated in ultrahigh vacuum with a base pressure $<1 \times 10^{-10}$ Torr. An n-type Si(111) wafer with a room-temperature resistivity of 7−10 Ω·cm was used as the substrate. It was cleaned and prepared using standard annealing procedures to form a well-reconstructed Si(111)-(7 × 7) surface. Ag was evaporated and deposited in situ on to the Si(111)-(7 × 7) surface at room temperature, while the STM tip was retracted a sufficient distance from the sample surface to avoid the tip shadowing effect. The deposition rate was kept at $\sim 2.1 \times 10^{-3}$ monolayer (ML) per

Received: August 20, 2010
Revised: January 24, 2011
Published: February 20, 2011

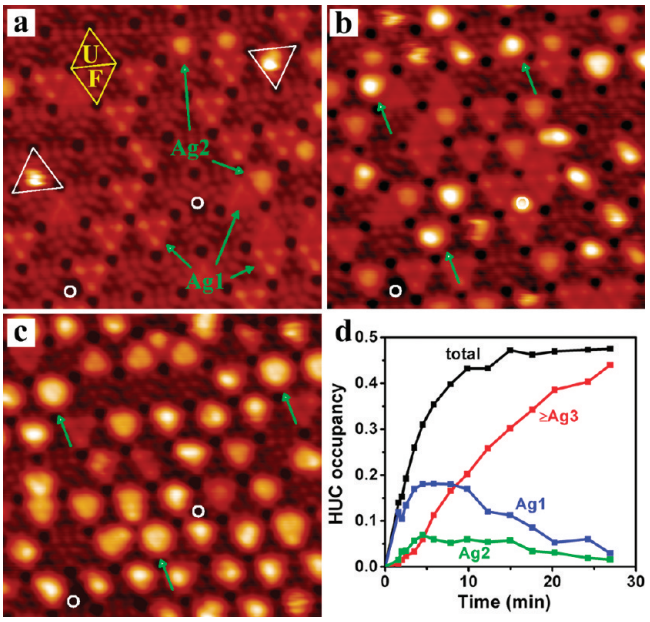

Figure 1. (a) STM image (19 nm × 18 nm) of a Si(111)-(7 × 7) surface after 2.5 min deposition of Ag. "F" and "U" represent a faulted half unit cell and an unfaulted half unit cell, respectively. Several one-Ag atom structures (Ag1) and two-Ag atom structures (Ag2) are indicated by arrows. Two intrinsic defects are labeled by small circles and provide position marks for the imaging areas. (b) and (c) are STM images of the same area as (a) with a total Ag deposition time of 10 and 27 min, respectively. The arrows in both cases indicate one kind of Ag structure repeatedly found in the HUCs. (d) The deposition time dependence of the HUC occupancy of various Ag structures.

minute (1 ML = 7.83 × 10^{14} atoms/cm^2). With a very small drift, the STM imaging could be conducted at the same sample area before and after the deposition of Ag atoms. Several deposition-imaging cycles were carried out, thereby providing an STM movie of the Ag structure growth. To observe the diffusion and transformation of Ag structures formed on Si(111)-(7 × 7), continuous images were also taken at the same area for certain Ag coverage. Unless otherwise specified, all the images were taken at room temperature.

In this study, the STM images were taken at a sample bias of +2 V and a tunneling current ~0.05 nA. The choice of a +2 V sample bias is to enable all the Ag structures to be observable. Due to the reported rectification effect on Ag clusters,[45] the current response from the Ag structures at lower bias voltages or negative bias voltages is usually small, which renders some Ag structures to lose contrast from the Si surface, or even disappeared in the STM image.[49] The small tunneling current of ~0.05 nA used in our experiment is to place the STM tip relatively far away from the surface to minimize the electrical effect of the STM tip on the observed features.[43] This current value is sufficiently small since imaging at a high tunneling current (but still <1 nA) yields almost the same STM images of the Ag structures with no change or damage to the Ag structures. This is consistent with the results by P. Sobotik et al.[42] who have shown that a tunneling current <0.35 nA does not affect the inter-HUC diffusion of Ag1 structures.

RESULTS AND DISCUSSION

Growth Kinetics. Figure 1 shows the results from the 14 deposition-imaging cycles of the same sample area of 60 nm × 60 nm. Panels (a), (b), and (c) show three STM images with a total deposition time of 2.5, 10, and 27 min, respectively. As shown in Figure 1(a), when the coverage is relatively low (2.5 min corresponds to ~0.006 ML), most of the Ag atoms in HUCs form Ag1 (Ag monomer) and Ag2 (Ag dimer) structures, as indicated by the arrows. Their morphologies in STM images result from one- or two-Ag atom hopping within the HUCs at a much faster rate than the scanning speed of the STM tip and thus represent their characteristic time-averaged STM images.[42−44] In this paper, a Ag structure in a HUC containing *n* Ag atoms is donated by Ag*n*. If the type of the HUC is distinguished, it is donated by *n*F or *n*U for *n* Ag atoms in FHUC and UHUC, respectively. For the isomers with the same number of Ag atoms, an apostrophe is added to distinguish them. Besides these well-known Ag1 and Ag2 structures, two new bright features (labeled by the triangles) were found in this image. They were not found at lower coverages and would appear more frequently at higher coverages. Increasing Ag coverage showed other types of structures. The arrows in Figure 1(b) and 1(c) indicate two new types of structures that, respectively, started to form after ~4 min (0.009 ML) and ~15 min (0.03 ML) Ag deposition. Each of these new Ag structures contains more than two Ag atoms.

Figure 1(d) shows the HUC occupancy for various Ag structures as a function of total deposition time. The statistics are from ~1000 HUCs. The HUC occupancy by Ag1 and Ag2 increases initially, reaches its maximum at ~4 min, and starts to decrease afterward. In contrast, the HUC occupancy by structures with more than 2 Ag atoms shows a continuous increase. The total HUC occupancy nearly reaches a saturation value after ~15 min deposition since the new incoming Ag atoms tend to diffuse into the neighboring Ag structures and increase their size.[34,50]

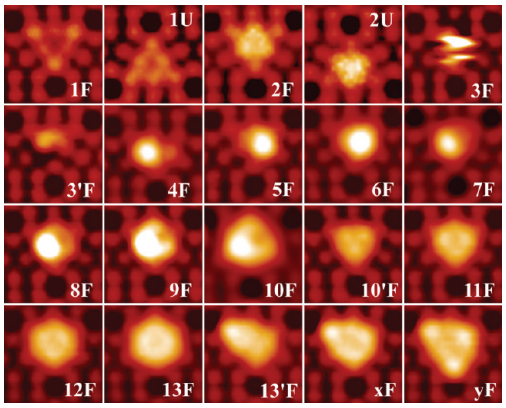

Figure 2. STM images of typical Ag structures formed in half unit cells with increasing size. F and U represent the Ag structure formed in the faulted half unit cell and the unfaulted half unit cell, respectively. The number in each label represents the number of Ag atoms in the structure. The number of Ag atoms in *x*F and *y*F was not identified. The apostrophe used after a number serves to label the isomer with the same number of Ag atoms.

STM Images of Typical Ag Structures. To further classify the Ag structures within each HUC, we show their zoom-in images in Figure 2 for various Ag configurations in FHUC, observed at different coverages up to the point where isolated Ag structures in a HUC are no longer identifiable. The Ag1 and Ag2 in UHUC are also shown in Figure 2 as 1U and 2U, respectively, for the purpose of comparison. The sequence of these structures is arranged according to the coverage sequence at which the Ag structure appears. As stated before, the numbers in the labels represent the number of Ag atoms contained in these structures, as we will demonstrate later, while F and U represent the types of

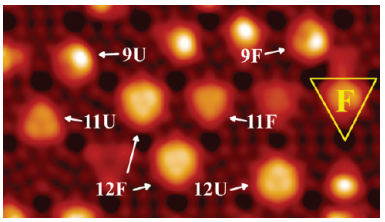

Figure 3. STM image comparing several Ag structures containing the same number of Ag atoms in FHUC and UHUC. The triangle labels a FHUC.

HUC where the Ag structures are located. The structures from 1F to 13F in Figure 2 are unique and could easily be distinguished from other structures. However, *x*F to *y*F have a number of similar structures but not shown here, and thus the numbers of Ag atoms inside *x*F and *y*F together with their similar structures are not determined.

There are clear differences among the structures from 1F to 13F as shown in the STM images. Contrary to what one might expect, the brightness of the structures does not seem to be monotonic with the number of Ag atoms. 1F and 1U appear as bright triangular patterns due to the fast motion of the single Ag atom within the half unit cells. The difference occurs at the three center Si-adatom sites which look brighter for 1U than for 1F. This difference is due to the asymmetric hopping motions of Ag in the two kinds of HUCs.[42] Similarly, 2U shows brighter spots at the three center Si-adatom sites than 2F. This is also attributable to the difference of Ag atom hopping motions. The Ag atoms in 3F are mobile at room temperature but move at a slower rate than those in 1F and 2F. Their hopping rate is comparable with the scanning line speed, resulting in the fuzzy features in the STM image. From 3′F to *y*F, all structures could yield stable STM images at room temperature. With respect to the underlying HUC of Si(111)-(7 × 7), the structures of 3′F, 4F, 5F, and 6F have no axis of symmetry; 7F, 8F, 9F, 10F, 13′F, *x*F, and *y*F have one axis of symmetry; while 10′F, 11F, 12F, and 13F have three axes of symmetry.

Some of the differences between room-temperature structures lie almost entirely in the contrast of the image. For example, 6F looks larger and brighter than 5F in the same image. But if the contrast is adjusted separately in the images, they may look quite the same. This kind of similarity also occurs for 8F and 9F and for 10F, 11F, and 12F. The sequence of brightness for each panel in Figure 2 is maintained, but the contrast may be different to display the individual structures well.

Each structure from 3F to 12F in Figure 2 has a counterpart in UHUC, which looks almost the same if the orientations of FHUC and UHUC are rotated. Figure 3 shows an STM image including 9F, 11F, and 12F together with their counterparts 9U, 11U, and 12U. Aside from a small contrast difference, each pair of counterparts looks identical. As mentioned above, 11F and 12F mainly differ in contrast and are easily distinguished within the same STM image (Figure 3). The contrast difference between 12F and 12U is negligible compared to that between 12F and 11F. The UHUC counterparts from 13F to *y*F were not observed in our attempts. However, they are believed to exist at higher coverages. It is simply too difficult to identify them due to the crowded structures at high coverages.

Intra-HUC Diffusion. While structures from 3′F to *y*F and 3′U to 12U remain stable at room temperature for STM imaging, hopping of the Ag atoms inside the same HUCs was still observable. Figure 4 demonstrates two sets of hopping events,

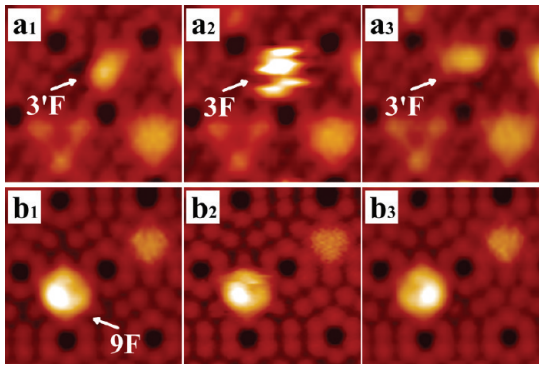

Figure 4. $(a_1)-(a_3)$ Transformation between 3′F and 3F structures. $(b_1)-(b_3)$ Transformation of a 9F to its equivalent configuration.

one for 3′F and the other for 9F. In Figure 4(a1) and (a3), we can clearly see the structure of 3′F at different orientations. During the transformation, 3′F first transforms to a 3F structure and then back to 3′F with its orientation rotated by 120°. The 3F structure is mobile and looks much brighter than 3′F. With no changes in the surrounding areas, the transformation between 3F and 3′F indicates that they contain the same number of Ag atoms but with different kinds of structure. This type of transformation also takes place between 13F and 13′F. 10F (10U) was observed to transform to 10′F (10′U), but no reverse transformation was observed. This type of transformation has allowed us to identify the above isomeric structures.

Figure 4(b1) and (b3) are two 9F images that have rotated within the half unit cell by 120°. Figure 4(b2) records a hopping event as the fussy noise when such a transformation occurs. This kind of structure rotation is quite common, as was also observed for 4F, 6F, 7F, and 8F structures and their counterparts in UHUC, for which no isomeric structures exist.

Inter-HUC Diffusion and Identification of the Number of Ag Atoms within a Ag Structure. At room temperature, we also observed inter-HUC diffusion, although the frequency was much lower than the intra-HUC diffusion described above. On the basis of the inter-HUC diffusion of Ag atoms, we can determine the number of Ag atoms in a given structure.[34,42] Figure 5 shows examples of four sets of inter-HUC diffusion events. Panels (a1) to (a3) show a transformation from a 2F structure to a 3′F structure and the concomitant diffusion of a 1F structure. As there were no changes in the surrounding areas, we can conclude that the Ag atom in 1F in panel (a1) first diffused into the neighboring UHUC to form the 1U structure in panel (a2), and finally this 1U structure merged with the 2F structure to form a 3′F structure. Panels (b1) to (b5) show the growth process of a 3′F structure (b1) to a 4F structure (b3) and finally to a 5F structure (b5). In Figure 5(b2), a Ag atom of 1F is observed to diffuse upward to an UHUC, as shown by the sudden image line change indicated by the horizontal dashed line. This diffusion event is also evident by the image of a partial trace of a 1U structure that now appeared in the neighboring UHUC, as indicated by the arrow (the scanning direction is from bottom to top). The 1U Ag atom quickly diffuses into the neighboring 3′F structure to form a 4F structure, as shown in Figure 5(b3). A similar process occurs in Figure 5(b4), where the 1F Ag atom first hops to the next UHUC and finally merges with the 4F structure to form a 5F structure, as shown in Figure 5(b5). The horizontal dashed line in Figure 5(b4) indicates the scanning line at

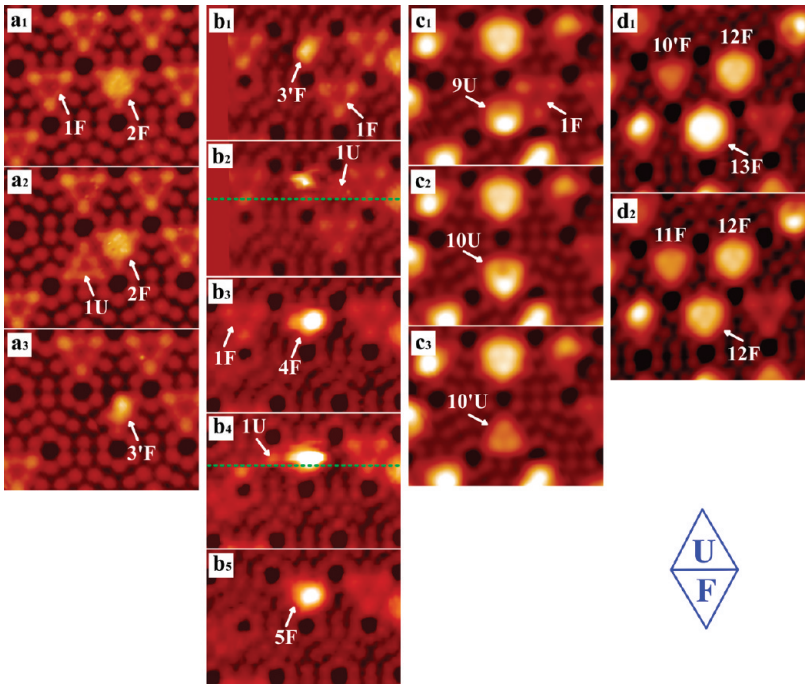

Figure 5. $(a_1)-(a_3)$, $(b_1)-(b_5)$, and $(c_1)-(c_3)$ are three sets of consecutive images showing the diffusion of a single Ag atom that induces the transformation of Ag structures. In (b_2) and (b_4), the horizontal dashed lines label the scanning lines at which the Ag atom makes a hop, and the "1U" labels the partial STM image of the Ag1 features after the hop. $(d_1)-(d_3)$ are the simultaneous transformations of two Ag structures in consecutive images with no other transformations in the surrounding area. "F" and "U" label the faulted half unit cell and the unfaulted half unit cell, respectively.

which the hopping event of a Ag from FHUC to UHUC takes place. The above observations can be expressed as

$$2F + 1U \rightarrow 3'F \quad (1)$$

$$3'F + 1U \rightarrow 4F \quad (2)$$

$$4F + 1U \rightarrow 5F \quad (3)$$

Figure 5(c1) to (c3) shows an example for the Ag structures in UHUC. A 1F structure is next to a 9U structure in Figure 5(c1). In the next image, as shown in Figure 5(c2), this 1F merges into the 9U and disappears, while the 9U structure is transformed into a 10U structure. The 10U structure is not stable and quickly turns into a 10′U structure without any changes in the surrounding structures, as shown in Figure 5(c3). The following expression can be obtained for these processes

$$9U + 1F \rightarrow 10U \rightarrow 10'U \quad (4)$$

Figure 5(d1) and (d2) demonstrates an example of yet another kind of diffusion event. While the Ag structures in the surrounding area show no changes, the images of the 10′F and 13F structures change simultaneously and end up as 11F and 12F structures, respectively. Such a change can be achieved through the diffusion of a single Ag atom from 13F to 10′F via intermediate states, though the diffusion event of the Ag atom has not been recorded here. This simultaneous transformation can be expressed by

$$10'F + 13F \rightarrow 11F + 12F \quad (5)$$

By making a large number of observations of inter-HUC diffusion events, we have obtained many expressions similar to eqs 1−5. Most of these expressions are related to the diffusion of a single Ag atom and have the form of eq 3. The number of Ag atoms in each structure could therefore be determined from these expressions. For example, from eq 1 to eq 3, the number of Ag atoms of 3′F, 4F, and 5F can be deduced as 3, 4, and 5, respectively. In this way, even though the STM images are not able to resolve individual Ag atoms in the Ag structures, we have identified the numbers of Ag

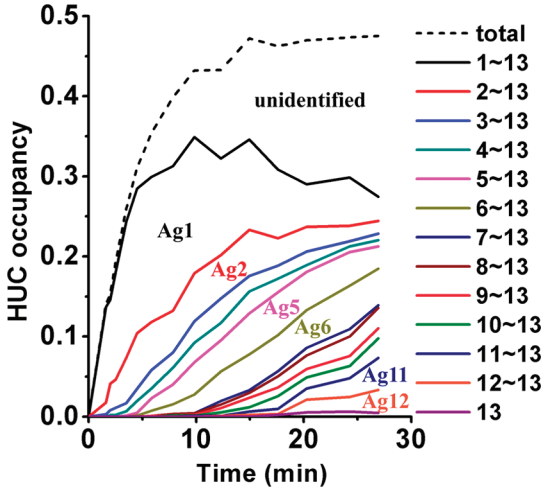

Figure 6. Time evolution of HUC occupancy of Ag structures. The dashed line shows the occupancy of all Ag structures, while the solid line shows the occupancy of Ag structure with the number of Ag atoms between various intervals, from [1,13] to [13,13]. For example, the top solid line represents the occupancy of identified Ag structures with 1−13 Ag atoms. The spaces between the two nearest solid lines demonstrate the occupancy of structures with the same number of Ag atoms. Ag1, Ag2, Ag5, Ag6, Ag11, and Ag12 are labeled in their respective spaces. The space between the dashed line and the top solid line represents those Ag structures with an unidentified number of Ag atoms.

dx.doi.org/10.1021/jp107921c |J. Phys. Chem. C 2011, 115, 3847–3853

Table 1. Transformation Events of Ag Structures Observed in Successive STM Images[a]

Δn \ Ag n (Count)	0	1	2	3	4	5	6	7	8	9	10	11	12	13
+2													-	-
+1	4	2	2		1	3	1	3	8	4	8	2	6	-
0	5K	272	135	78	74	371	443	82	178	195	174	322	221	76
-1	-	30											4	4
-2	-	-	1											1

[a] A series of STM images are acquired at the same Ag coverage at room temperature. Transformations of recognized Ag structures between consecutive STM images are counted. The first row (Ag n) labels the number of Ag atoms in a Ag structure before its transformation, while the first column labels the transformation result in terms of the change of the number of Ag atoms (Δn). For example, the number "30" in column "$n = 1$" means that 30 events are observed for the Ag1 structures to become Ag0 (empty, $\Delta n = -1$) in the next image. The empty cells in the table are all zeros. The dark gray cells are the counts of unchanged events, and the light gray cells mark the nonzero counts of the transformation events.

atoms in all the structures from 3F to 13′F and from 3U to 12U and have labeled the number of Ag atoms in their notations. The number of atoms in Ag structures in FHUC and UHUC were determined independently, and no conflict was found.

The number of Ag atoms in structures labeled by xF and yF in Figure 2 were not identified because of the difficulty of distinguishing them among various similar structures. They appear sequentially after 13F (13′F) at higher coverages. Thus, the number of atoms of xF and yF should be at least 14 and 15, respectively. The maximum number of Ag atoms accommodated in a HUC is thus at least 15. This agrees with the estimation made earlier by P. Kocán et al.[40]

Having identified the number of Ag atoms in each Ag structure, we can now plot their time dependence during Ag deposition. Solid lines in Figure 6 show the occupancy evolution of the identified Ag structures. For clarity, the top solid line represents occupancy of HUC by all the identified Ag structures containing 1−13 Ag atoms, the second top solid line represents occupancy of HUC by all identified Ag structures containing 2−13 Ag atoms, etc. Thus, the difference between the top solid line and the second top solid line represents the occupancy of the Ag1 structure. The occupancy of the other Ag structures can be deduced in a similar manner. These curves show a complex growth process of the Ag structures. The occupancy of structures Ag1 to Ag4 rises at first, reaches a maximum after around 5 min (∼0.01 ML), and then decreases. The occupancy of structures Ag3 and Ag4 is obviously smaller than that of Ag5 and Ag6 after a deposition time of 5 min, while structures of Ag11 and Ag12 also show a relatively larger occupancy after a deposition time of 20 min. These features are closely related to the diffusion dynamics of the Ag atoms which we will discuss later. The low occupancy of Ag7 is partly due to its fast intra-HUC hopping, which renders the STM image unrecognizable.

The dashed line in Figure 6 is the total HUC occupancy of Ag structures which was already shown in Figure 1(d). It is significantly larger than the top solid line after 5 min Ag deposition. This is due to a large number of Ag structures with unidentified number of Ag atoms. With a detailed inspection of the unidentified structures in the STM image after 27 min Ag deposition, we could attribute them to the following reasons: (1) about 25% unidentifiable Ag structures connect with neighboring Ag structures; (2) about 30% unidentified Ag structures are due to a hopping feather like Figure 4(b2); (3) about 8% of the HUCs with unidentified structures contain more than 13 Ag atom numbers, such as xF and yF in Figure 2; and (4) about 37% are nontypical Ag structures. Their configurations appear very rare on the surface and have not been identified yet. One cause for these nontypical structures could be the metastable Ag structures. Another cause, which is more important, is the Si defects or interactions with the Si in HUCs. Although intrinsic defects before Ag deposition were marked and avoided in statistics, new defects might emerge during the deposition and the growing process of Ag structures. These defects and transformations could induce nontypical Ag structures.

Stability of Ag Structures. To evaluate the size stability of the Ag structures at room temperature, after a total of 27 min Ag deposition, we have taken 17 images over the same surface areas with a time interval of 10.5 min between each. In Table 1 the initial number of Ag atoms in each structure is shown in the top row. The statistics of the changes in the next sequential images are summarized in the body of the table: As one can see, a dominant number of structures stay unchanged in the next STM image ($\Delta n = 0$). Up to $n = 11$ atoms, the Ag structures are stable against dissociation. The decrease of the number of atoms for Ag1 and Ag2 structures in the table is due to their diffusion as an entity to the neighboring HUCs, empty or with a large Ag structure. For Ag3 to Ag11 structures, they are so stable that their Ag atoms do not diffuse to the neighboring HUCs. For Ag12 to Ag13 structures, events of dissociation by reducing the size with 1 to 2 Ag atoms are observed, indicating that the Ag13 structure can decay into the Ag12 structure and that the Ag12 structure can also automatically decay into the Ag11 structure. The instability of Ag12 and Ag13 structures leads to an accumulation of structures Ag11 and Ag12, respectively, and thus a larger occupancy in Table 1 and Figure 6. On the basis of the data in Table 1, we can semiquantitatively estimate the lifetime of the Ag structures against dissociation, as shown in the row "Dissociation" in Table 2. The lifetime of Ag12 and Ag13 is directly obtained by considering the dissociation probability in the time interval of 10.5 min, i.e., 4 dissociated events among a total of 225 observations for Ag12 and 5 dissociated events among a total of 81 observations for Ag13. For Ag3−Ag11, since no dissociation events are observed, we estimate the lower bound of their lifetimes by assuming one dissociation event among the respective observations.

When there is a Ag1 structure in the neighboring HUCs, most of these Ag structures are ready to capture it to grow bigger by $\Delta n = 1$. No event with $\Delta n = 2$ or larger is observed in the statistics. The disappearance of a neighboring Ag1 structure accompanied with the Ag structure growth is consistent with the reaction schemes we showed in Figure 5. Although all types of Ag structures can increase their sizes, there are still differences among their stabilities against association with the neighboring

Table 2. Measurement of the Dynamic Processes of Ag Structures[a]

Ag n / τ	3	4	5	6	7	8	9	10	11	12	13
Dissociation	>13 h	>13 h	>65 h	>77 h	>14 h	>31 h	>34 h	>30 h	>56 h	9.6 h	2.7 h
Association	2.6 m	1.2 m	13 h	4.6 h	13 m	15 m	9.5 m	3.1 m	2 m	6 s	-
Internal motion	0.8 s	0.9 s	>12 h	4 h	0.5 s	17 s	24 s	<1 ms	<1 ms	<1 ms	-

[a] Row "Dissociation" tabulates the lifetime against dissociation of the Ag*n* ($3 < n < 13$) structures. Row "Association" tabulates the average time for a Ag1 to immerge with a neighboring Ag*n* structure. Row "Internal motion" tabulates the average time of an internal hopping or vibration of the Ag*n* structures inside a HUC.

Table 3. Transformation Events of Ag Structures Observed in Successive STM Images at Various Ag Coverages[a]

Δn \ Ag n / Count	0	1	2	3	4	5	6	7	8	9	10	11	12	13
+6	2					2	2		-	-	-	-	-	-
+5	11	8	2			4	2	1		-	-	-	-	-
+4	8	4	5			6	6		3		-	-	-	-
+3	11	8	20	7	2	8	15	2	6	4	3	-	-	-
+2	70	30	19	23	15	6	24	1	12	9	11	4	-	-
+1	612	176	59	36	48	93	12	13	16	18	20	12	4	-
0	7K	820	256	66	49	134	112	6	21	10	16	16	14	2
-1	-	302	12							2		3	11	4
-2	-	-	35	1									1	1
-3	-	-	-	3										

[a] A series of 15 STM images are acquired at various Ag coverages as described in Figure 1. The table tabulates the transformation events of the Ag structures similar to Table 1.

Ag1 structure. By continuous STM imaging, the average time for the association of a Ag1 structure with a neighboring Ag3−Ag12 can be measured, and the results are shown by the row "Association" in Table 2. Most of the Ag structures can easily capture a neighboring Ag1 in several minutes, while Ag5 and Ag6 show a prominent longer time to do so. This difference could affect the growth process and the abundance of these structures. As shown in Table 1 and Figure 6, the numbers of Ag5 and Ag6 are much bigger than the numbers of Ag3 and Ag4, which is a result of faster Ag1 diffusions into a neighboring Ag3 or Ag4 structure than that into a neighboring Ag5 or Ag6 structure. The fast capture of Ag1 by Ag3 and Ag4 (growing into Ag4 and Ag5) in contrast to the slow capture of Ag1 by Ag5 and Ag6 (growing into Ag6 and Ag7), a result of their stability against association, makes the number of Ag5 and Ag6 to accumulate and have a longer lifetime. We must emphasize that continuous STM imaging with a Ag1 structure neighboring to the Ag structure of interest is important for obtaining the lifetime against association. In the statistics in Table 1, for many Ag structures, since there is no neighboring Ag1 to be captured, the number of events for growth is normally fewer than that predicted by the measured lifetime of association.

The statistical results presented in Table 3, which were taken from 15 STM images immediately after each additional Ag deposition, also demonstrated the dissociation and association stability we concluded from Table 1. The additional Ag atoms deposited from the source can directly increase the size of existing Ag structures or provide a large reservoir of Ag1 structures and thus lead to a continuous growth of Ag structures with $\Delta n \gg 1$. Occasionally, the incoming Ag atom may impinge on a Ag structure and cause it to dissociate, as evidenced by the increased number of dissociations listed in Table 3.

As we have discussed previously in Figure 4, even without inter-HUC diffusion of Ag atoms, Ag3, Ag10, and Ag13 structures can change automatically between their isomers. Structural rotation of Ag4 and Ag6−9 can also exist. These room-temperature STM images indicate the active hopping of their Ag atoms inside the HUC, although the number of Ag atoms has been retained. Table 2 also summarizes the average time of internal hopping motion for Ag3−Ag9 structures which are measured by continuous STM imaging. The structures of Ag3, Ag4, and Ag7−Ag9 hop frequently inside a HUC on a time scale of seconds, while Ag5 and Ag6 remain immobile for several hours. At low temperatures (e.g., 5 K), the Ag atom in 1F and 1U stops hopping and appears as a single bright spot within HUCs.[41] Ag atoms in 2F and 3F also stop hopping at 77K and show dimer and trimer structures in the STM images.[45] In our low-temperature measurements (STM images not shown here), Ag atoms in 3′F to *y*F structures in Figure 2 are all observed to fully stop hopping at temperatures at 80 K. In the low-temperature STM images, 10′F, 11F, and 12F, although quite stable at room temperature against atom hopping, look slightly different from their room-temperature counterparts, indicating the vibrational motion at room temperature for structures of 10′F, 11F, and 12F has also ceased at 80 K. They vibrate much faster than the STM scanning speed (∼1 ms for each point) at room temperature and do not induce any hopping feature in the STM image.

CONCLUSIONS

In summary, we have recorded the STM movie of the growth process of Ag structures on a Si(111)-(7 × 7) surface via a set of deposition-imaging cycles at room temperature. As the deposition time increased, the HUCs were found to form Ag atom traps and were occupied by various Ag structures with increasing numbers of Ag atoms. Up to the coverage where the neighboring Ag structures started to merge together, all the individual typical Ag structures in the HUCs were identified, and identical Ag structures were found to occupy both FHUC and UHUC. Through observing the transformations of different Ag structures induced by inter-HUC diffusion of Ag atoms, the number of Ag atoms in each Ag structure was identified, thus establishing relations between STM images and their numbers of Ag atoms from 1 to 13 for FHUC and from 1 to 12 for UHUC. To our knowledge, previous works only reported the relation up to 2 Ag atoms for Ag structures on Si(111)-(7 × 7). Clearly, the identification of the number of atoms in each Ag structure can provide a critical base for understanding their physical and chemical properties, although the detailed atomic configuration remains to be a future work. Our method is expected to be applicable for structures formed by other metals on a Si(111)-(7 × 7) surface.

AUTHOR INFORMATION

Corresponding Author

*E-mail: xdxiao@phy.cuhk.edu.hk. Tel.: (852) 3163-4388. Fax: (852) 2603-5204.

ACKNOWLEDGMENT

This work was supported by the Research Grants Council of Hong Kong (N_CUHK616/06) and the Natural Science Foundation of China (50618001).

REFERENCES

(1) de Heer, W. A. *Rev. Mod. Phys.* **1993**, *65*, 611.
(2) Binns, C. *Surf. Sci. Rep.* **2001**, *44*, 1.
(3) Baletto, F.; Ferrando, R. *Rev. Mod. Phys.* **2005**, *77*, 371.
(4) Wilcoxon, J. P.; Abrams, B. L. *Chem. Soc. Rev.* **2006**, *35*, 1162.
(5) Ferrando, R.; Jellinek, J.; Johnston, R. L. *Chem. Rev.* **2008**, *108*, 845.
(6) Schnockel, H. *Chem. Rev.* **2010**, *110*, 4125.
(7) Schmidt, M.; Kusche, R.; von Issendorff, B.; Haberland, H. *Nature (London)* **1998**, *393*, 238.
(8) Rytkönen, A.; Häkkinen, H.; Manninen, M. *Phys. Rev. Lett.* **1998**, *80*, 3940.
(9) Häkkinen, H.; Manninen, M. *Phys. Rev. Lett.* **1996**, *76*, 1599.
(10) Li, J.; Li, X.; Zhai, H. J.; Wang, L. S. *Science* **2003**, *299*, 864.
(11) Zheng, J.; Zhang, C.; Dickson, R. M. *Phys. Rev. Lett.* **2004**, *93*, 077402.
(12) Félix, C.; Sieber, C.; Harbich, W.; Buttet, J.; Rabin, I.; Schulze, W.; Ertl, G. *Phys. Rev. Lett.* **2001**, *86*, 2992.
(13) Xu, X.; Yin, S.; Moro, R.; de Heer, W. A. *Phys. Rev. Lett.* **2005**, *95*, 237209.
(14) Reveles, J. U.; Clayborne, P. A.; Reber, A. C.; Khanna, S. N.; Pradhan, K.; Sen, P.; Pederson, M. R. *Nat. Chem.* **2009**, *1*, 310.
(15) Fielicke, A.; Kirilyuk, A.; Ratsch, C.; Behler, J.; Scheffler, M.; von Helden, G.; Meijer, G. *Phys. Rev. Lett.* **2004**, *93*, 023401.
(16) Diederich, T.; Doppner, T.; Braune, J.; Tiggesbaumker, J.; Meiwes-Broer, K.-H. *Phys. Rev. Lett.* **2001**, *86*, 4807.
(17) Häkkinen, H.; Moseler, M.; Kostko, O.; Morgner, N.; Hoffmann, M. A.; Issendorff, B. v. *Phys. Rev. Lett.* **2004**, *93*, 093401.
(18) Chiu, Y. P.; Huang, L. W.; Wei, C. M.; Chang, C. S.; Tsong, T. T. *Phys. Rev. Lett.* **2006**, *97*, 165504.
(19) Bartels, C.; Hock, C.; Huwer, J.; Kuhnen, R.; Schwöbel, J.; von Issendorf, B. *Science* **2009**, *323*, 1323.
(20) Assadollahzadeh, B.; Schwerdtfeger, P. *J. Chem. Phys.* **2009**, *131*, 064306.
(21) Gruene, P.; Rayner, D. M.; Redlich, B.; van der Meer, A. F. G.; Lyon, J. T.; Meijer, G.; Fielicke, A. *Science* **2008**, *321*, 674.
(22) Reveles, J. U.; Sen, P.; Pradhan, K.; Roy, D. R.; Khanna, S. N. *J. Phys. Chem. C* **2010**, *114*, 10739.
(23) Roach, P. J.; Woodward, W. H.; Castleman, A. W.; Reber, A. C., Jr.; Khanna, S. N. *Science* **2009**, *323*, 492.
(24) Reber A, C.; Khanna, S. N.; Roach, P. J.; Woodward, W. H.; Castleman, A. W., Jr. *J. Phys. Chem. A* **2010**, *114*, 6071.
(25) Roach, P. J.; Woodward, W. H.; Reber, A. C.; Khanna, S. N.; Castleman, A. W., Jr. *Phys. Rev. B* **2010**, *81*, 195404.
(26) Lopez-Acevedo, O.; Kacprzak, K. A.; Akola, J.; Häkkinen, H. *Nat. Chem.* **2010**, *2*, 329.
(27) Arenz, M.; Landman, U.; Heiz, U. *ChemPhysChem* **2006**, *7*, 1871.
(28) Turner, M.; Golovko, V. B.; Vaughan, O. P. H.; Abdulkin, P.; Berenguer-Murcia, A.; Tikhov, M. S.; Johnson, B. F. G.; Lambert, R. M. *Nature (London)* **2008**, *454*, 981.
(29) van Leonen, E. J.; Iwami, M.; Tromp, R. M.; van der Veen, J. F. *Surf. Sci.* **1984**, *137*, 1.
(30) Tosch, St.; Neddermeyer, H. *Phys. Rev. Lett.* **1988**, *61*, 349.
(31) Wan, K. J.; Lin, X. F.; Nogami, J. *Phys. Rev. B* **1993**, *47*, 13700.
(32) Gavioli, L.; Kimberlin, K. R.; Tringides, M. C.; Wendelken, J. F.; Zhang, Z. Y. *Phys. Rev. Lett.* **1999**, *82*, 129.
(33) Matsuda, I.; Ohta, T.; Yeom, H. W. *Phys. Rev. B* **2002**, *65*, 085327.
(34) Ošťádal, I.; Kocán, P.; Sobotík, P.; Pudl, J. *Phys. Rev. Lett.* **2005**, *95*, 146101.
(35) Kocán, P.; Ošťádal, I.; Sobotík, P. *Surf. Sci.* **2006**, *600*, 3928.
(36) Schmeidel, J.; Pfnür, H.; Tegenkamp, C. *Phys. Rev. B* **2009**, *80*, 115304.
(37) Sawa, K.; Aoki, Y.; Hirayama, H. *Phys. Rev. Lett.* **2010**, *104*, 016806.
(38) Takayanagi, K.; Tanishiro, Y.; Takahashi, S.; Takahashi, M. *Surf. Sci.* **1985**, *164*, 367.
(39) Vitali, L.; Ramsey, M. G.; Netzer, F. P. *Phys. Rev. Lett.* **1999**, *83*, 316.
(40) Kocán, P.; Sobotík, P.; Ošťádal, I.; Kotrla, M. *Phys. Rev. B* **2004**, *69*, 165409.
(41) Zhang, C.; Chen, G.; Wang, K.; Yang, H.; Su, T.; Chan, C. T.; Loy, M. M. T.; Xiao, X. *Phys. Rev. Lett.* **2005**, *94*, 176104.
(42) Sobotík, P.; Kocán, P.; Ošťádal, I. *Surf. Sci.* **2003**, *537*, L442.
(43) Wang, K.; Chen, G.; Zhang, C.; Loy, M. M. T.; Xiao, X. *Phys. Rev. Lett.* **2008**, *101*, 266107.
(44) Lin, X.; Zhou, Y.; Li, J.; Wu, Q. *J. Comput. Theory Nanosci.* **2010**, *7*, 600.
(45) Hu, S.; Zhao, A.; Kan, E.; Cui, X.; Zhang, X.; Ming, F.; Fu, Q.; Xiang, H.; Yang, J.; Xiao, X. *Phys. Rev. B* **2010**, *81*, 115458.
(46) Li, J.-L.; Jia, J.-F.; Liang, X.-J.; Liu, X.; Wang, J.-Z.; Xue, Q.-K.; Li, Z.-Q.; Tse, J. S.; Zhang, Z.; Zhang, S. B. *Phys. Rev. Lett.* **2002**, *88*, 066101.
(47) Kotlyar, V. G.; Zotov, A. V.; Saranin, A. A.; Kasyanova, T. V.; Cherevik, M. A.; Pisarenko, I. V.; Lifshits, V. G. *Phys. Rev. B* **2002**, *66*, 165401.
(48) Byun, J. H.; Shin, J. S.; Kang, P. G.; Jeong, H.; Yeom, H. W. *Phys. Rev. B* **2009**, *79*, 235319.
(49) Sobotík, P.; Ošťádal, I.; Kocán, P. *Vacuum* **2004**, *76*, 465.
(50) Vasco, E.; Polop, C.; Rodríguez-Cañas, E. *Phys. Rev. B* **2003**, *67*, 235412.